Arch. Metall. Mater. **65** (2020), 3, 1041-1044

DOI: 10.24425/amm.2020.133214

SEONG YU YOON[1], BYUNG JOON CHOI[1,2*]

ELECTRICAL CHARACTERISTICS OF TIN OXIDE FILMS GROWN BY THERMAL ATOMIC LAYER DEPOSITION

Tin dioxide (SnO_2) is an n-type semiconductor and has useful characteristics of high transmittance, excellent electrical properties, and chemical stability. Accordingly, it is widely used in a variety of fields, such as a gas sensor, photocatalyst, optoelectronics, and solar cell. In this study, SnO_2 films are deposited by thermal atomic layer deposition (ALD) at 180°C using Tetrakis(dimethylamino) tin and water. A couple of 5.9, 7.4 and 10.1nm-thick SnO_2 films are grown on SiO_2/Si substrate and then each film is annealed at 400°C in oxygen atmosphere. Current transport of SnO_2 films are analyzed by measuring current – voltage characteristics from room temperature to 150°C. It is concluded that electrical property of SnO_2 film is concurrently affected by its semiconducting nature and oxidative adsorption on the surface.

Keywords: atomic layer deposition, tin oxide, electrical property, oxygen adsorption

1. Introduction

SnO_2 is widely used in the various applications, such as gas sensors, transparent electrodes and solar cells [1-4]. Such versatile usages are owing to its useful characteristics, for instance, wide band gap energy (~3.62eV) and high optical transmittance (~90%) and good electrical conductivity (0.1-89 Ω cm). When it comes to its gas sensor application, in particular, oxygen adsorption on the surface of SnO_2 plays a major role in the accumulation/depletion of electrons, which influences on the electrical conductivity [5,6].

SnO_2 films have been researched with numerous techniques including spray pyrolysis [7], pulsed-laser deposition (PLD) [8], chemical vapor deposition (CVD) [9]. Atomic layer deposition (ALD), which is upcoming technology and recently comes to use in various fields, is feasible to control a layer thickness as atomic units and figures lower temperature process, excellent step coverage in thickness and composition. Therefore, ALD-grown SnO_2 could be used for the new application. N. H. Lee et al. reported that ALD-grown SnO_2 film could be used as a robust friction layer for the triboelectric generator [10]. D.H. Kim et al. reported that SnO_2 layer coated on the surface of carbon nanofibers by ALD could enhance the current efficiency by adopting the direct methanol fuel cells [11]. Especially, SnO_2 with ALD technology is properly applied to a gas sensor due to various merits. In our prior work, we deposited SnO_2 film by using ALD and observed the decrease of the growth rate with increasing substrate temperature, at the same time, the density of the film was decreased with increasing temperature [12].

In this study, we performed the experiments with ALD-grown and annealed SnO_2 films and analyzed its current transport characteristics at the various temperatures. Based on these results, we investigated the traits according to the thickness of layers and temperature effect on the electrical properties of as-deposited and annealed SnO_2 films.

2. Experimental

The film growth was performed with horizontal traveling-wave-type reactor (Atomic Classic, CN-1 Co., KOREA). TDMA-Sn (Tetrakis(dimethylamino)tin) (UPCHEM Co., KOREA) and water were used as the metalorganic precursor and oxidant, respectively. The substrate temperature was kept at mainly 180°C. Nitrogen (high purity of 99.9999%) gas was used to control the working pressure with 0.7 mTorr during deposition as well as the purging gas. Figure 1 shows the schematics and time sequence of an overall ALD SnO_2 process. TDMA-Sn

---

[1] SEOUL NATIONAL UNIVERSITY OF SCIENCE AND TECHNOLOGY, DEPARTMENT OF MATERIAL SCIENCE AND ENGINEERING 01811SEOUL, KOREA
[2] SEOUL NATIONAL UNIVERSITY OF SCIENCE AND TECHNOLOGY, THE INSTITUTE OF POWDER TECHNOLOGY, 01811SEOUL, KOREA

* Corresponding author: bjchoi@seoultech.ac.kr

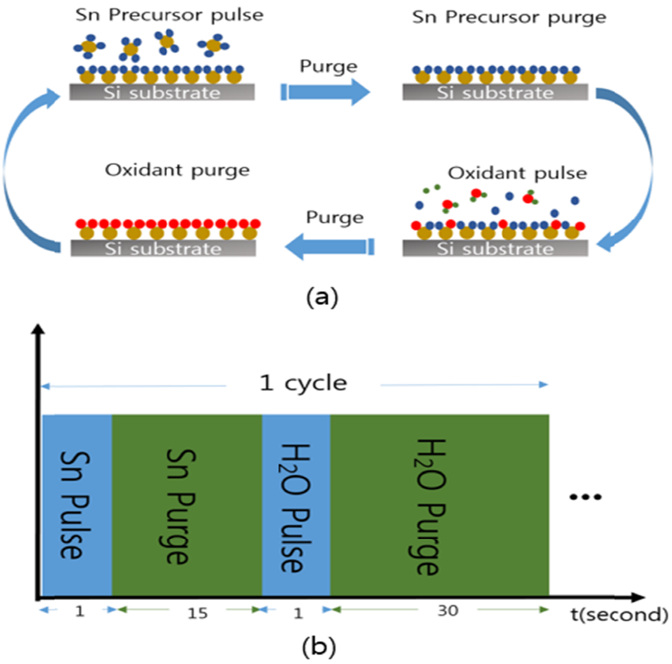

Fig. 1. (a) Schematics of ALD process (b) ALD pulse sequence

was carried by 50SCCM of N_2 gas, while H_2O was introduced by vapor draw. The film thickness was measured by spectroscopic ellipsometer (MG-1000, NANOVIEW, KOREA), where 350-840 nm range of visible light was used to obtain the spectra of refractive index from the samples.

SnO_2 were deposited 60, 90, and 120 cycles by ALD on thermally grown SiO_2/Si substrate. Each film was annealed with electric furnace at 400°C in air. The crystallinity of the films was analyzed by X-ray diffraction (XRD).

Figure 2 shows the device schematics for measuring current transport. Al electrode was deposited by e-beam evaporation via shadow mask on SnO_2/SiO_2/Si. The area between two Al electrodes was considered as the part of the current passing through. By doing so, specific resistance was calculated by using this area. Resistivity can be calculated from the resistance of the film and its dimension (d, t, and l). Semiconductor parameter analyzer (HP-4155A, AGILENT, USA) was used to analyze electrical characteristics of SnO_2 thin films by measuring current-voltage (I-V) hysteresis varying the substrate temperature from room temperature to 150°C.

3. Results and discussion

A sequence of ALD reaction is composed of TDMA-Sn feeding – purging – H_2O feeding – purging pulse as shown in Fig. 1. The linear growth rate of SnO_2 was about 0.9Å/cycle from 25 to 100 cycles at 180°C. Since we wanted to see the change of electrical properties according to the film thickness, SnO_2 ALD was done 60, 90, 120 cycles, which thickness was determined as 5.9, 7.4, and 10.1 nm, respectively.

Figure 3 shows the XRD spectra of 5 nm-thick as-deposited and annealed SnO_2 thin films grown on bare Si substrate. No other peak was observed in as-deposited SnO_2 samples as shown in Fig. 3(a). On the contrary, Fig. 3(b) show (110), (101), (200) peaks of SnO_2 positioned at 26, 34, 39 degrees, respectively.

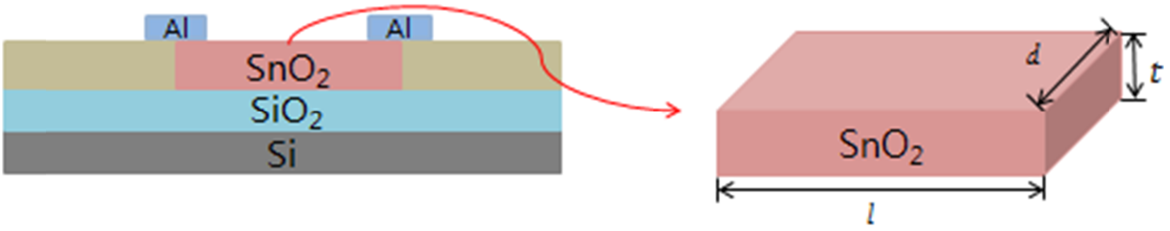

Fig. 2. Schematics of the fabricated samples for current transport

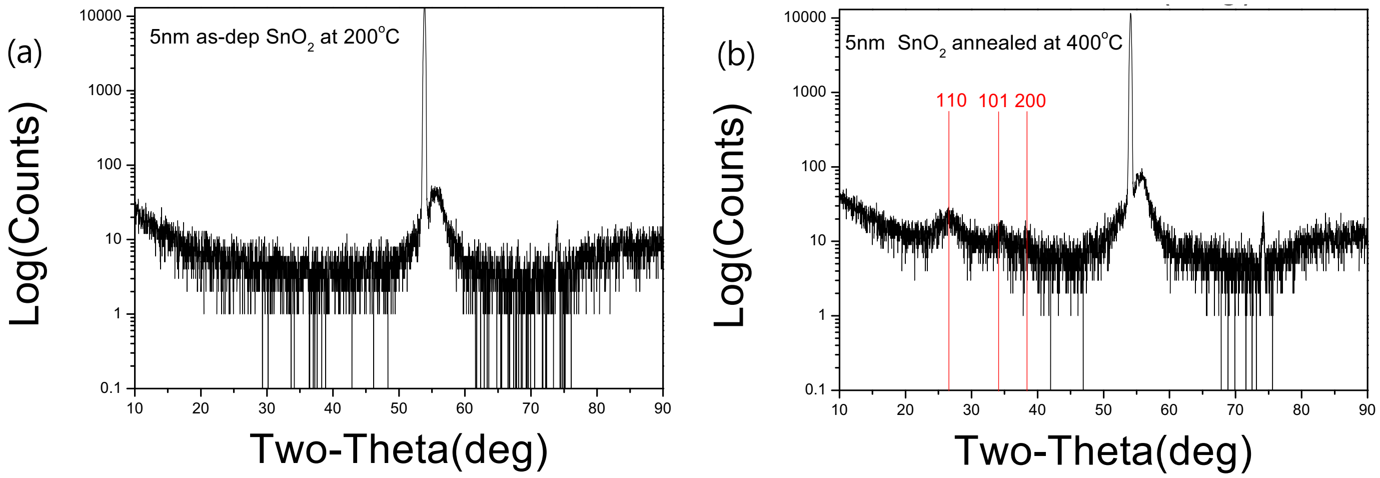

Fig. 3. XRD patterns of 5 nm-thick SnO_2 thin films (a) as-deposited and (b) annealed at 400°C

Therefore, as-deposited film has an amorphous phase and it could be crystallized with 400°C annealing in air.

I-V curves and resistivity of the as-deposited and annealed samples measured at room temperature are shown in Figure 4. As the films are thicker, current level becomes higher and more stable in Fig. 4(a). In addition, annealed films show higher current compared to that of as-deposited films. Fig. 4(b) exhibits the resistivity as a function of the film thickness based on I-V curves in Fig. 4(a). Resistivity was decreased by increasing film thickness. It is considered that surface depletion layer that does not contribute the current transport is similar with the samples in the same measurement condition so that thicker film significantly increase the carrier density in the film leading to the decrease of resistivity. Annealed films have lower resistivity compared to as-deposited samples. After annealing treatment, SnO_2 films became crystallized and its grain size became bigger. In general, electron is scattered by amorphous structure with short range order. Therefore, charge carriers (electrons) could have an unconstrained movement in the annealed film, which means the increase of charge density and mobility leading to the decrease of electrical resistivity. Note that the resistivity change after annealing is the largest in the case of 7.4 nm-thick SnO_2 samples. On the other hand, 5.9 nm SnO_2 samples were electrically unstable and showed little change after annealing. Although the film was crystallized, it was as thin as the depletion width on the surface by adsorbed H_2O and oxygen so that the amount of carrier was small.

Figure 5(a) and (b) show the trend of resistivity of 7.4 and 10.1 nm-thick as-deposited and annealed SnO_2 films under 4 different temperatures (60, 90, 120, 150°C) obtained from their I-V curves. Overall, annealed samples have lower resistivity in comparison with as-deposited samples as expected. Interestingly, resistivity was continuously decreased up to 120°C, but it was increased at 150°C in all samples. Decrease in the resistivity and negative temperature coefficient could be attributed to the generation of charge carriers in the semiconducting nature of

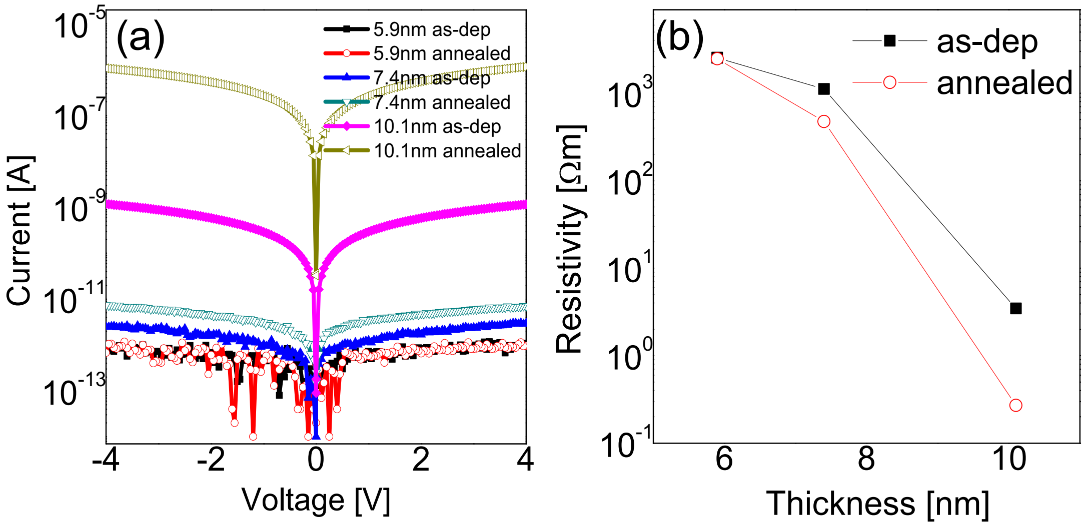

Fig. 4. Electrical properties of 5.9, 7.4, 10.1 nm-thick as-deposited and annealed samples. (a) I-V curves measured at room temperature (b) resistivity at room temperature

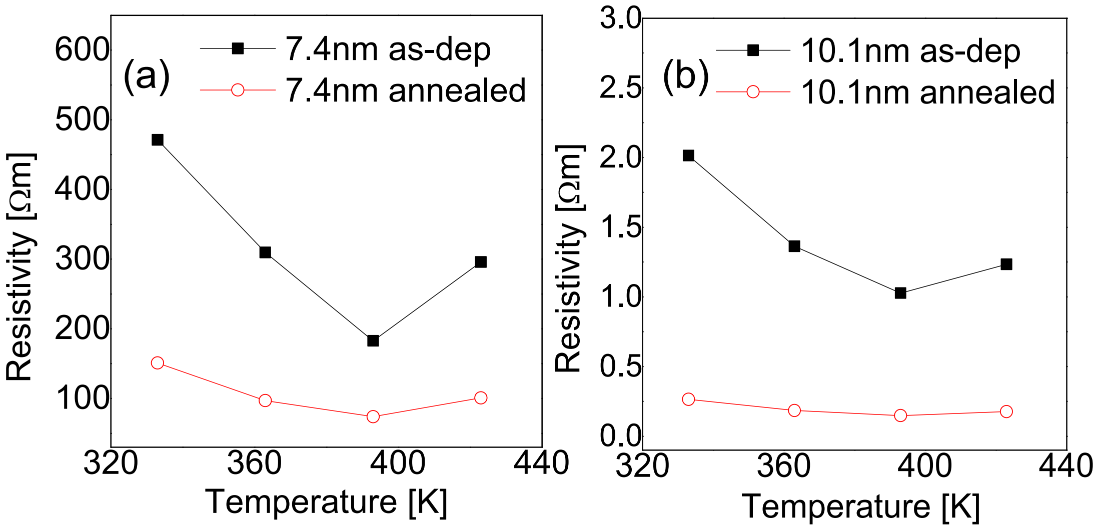

Fig. 5. Resistivity of (a) 7.4 and (b) 10.1 nm-thick as-deposited and annealed samples as a function of measurement temperature in K

SnO_2. However, adsorption of water and oxygen molecules on the surface of the film at the elevated temperature could increase the depletion width of SnO_2 surface, which results in the rebound of the resistivity at 150°C. In other words, oxidative adsorption makes larger depletion area, thereby leads to the interruption of carrier mobility and increase of electrical conductivity.

4. Conclusions

SnO_2 thin films were deposited by ALD with 0.9 Å/cycle at 180°C and their electrical characteristics were studied. As-deposited SnO_2 thin films were amorphous, while annealed films were crystallized at 400°C in air. Basic structure of samples was composed of $Al/SnO_2/SiO_2/Si$. 6 samples were fabricated with the 5.9, 7.4, and 10.1 nm-thick SnO_2 having as-deposited and annealed state. There was little resistivity change after annealing of 5.9 nm-thick SnO_2 samples. On the other hand, the resistivity of 7.4 and 10.1 nm-thick SnO_2 samples was largely reduced after annealing thanks to the crystallization. The resistivity of 7.4 and 10.1 nm SnO_2 was decreased with increasing temperature up to 120°C. However, resistivity was increased at 150°C. Such a change in the resistivity was considered as the competition between the semiconducting nature (negative temperature coefficient of resistivity) of SnO_2 film and oxidative adsorption (increase of depletion width) on the surface. These electrical characteristics of ALD-grown SnO_2 thin films could be used to optimize the thickness and resistivity range for its improved gas sensing application.

Acknowledgments

This study was supported by the Advanced Research Project funded by SeoulTech (Seoul National University of Science and Technology).

REFERENCES

[1] B. Orel, U.L. Stangar, K. Kalcher, J. Electrochem. Soc. **141**, 127 (1994).

[2] J.W. Leem, J.S. Yu, Mater. Sci. Eng. B **176**, 1207 (2011).

[3] B.Y. Wei, M.C. Hsu, P.G. Su, H.M. Lin, R.J. Wu, H.J. Lai, Sensors Actuators B **101**, 81 (2004).

[4] J.-W. Shin, S.-J. Choi, I.-K. Lee, D.-Y. Youn, C.-O. Park, J.-H. Lee, H.L. Tuller, I.-D. Kim, Adv. Funct. Mater. **23**, 2357 (2013).

[5] M. Habgood, N. Harrison, Surface Science **602**, 1072 (2008).

[6] U. Pulkkinen, T. T. Rantala, T. S. Rantala, V. Lantto, J. Molecular Catalysis A **166**, 15 (2001).

[7] G. Korotchenkov, V. Brynzari, S. Dmitriev, Sensors Actuators B **54**, 197 (1999).

[8] H. Kim, A. Pique, Appl. Phys. Lett. **84**, 218 (2004).

[9] J. Sundqvist, M. Ottosson, A. Harsta, Chem. Vap. Depos. **10**, 77 (2004).

[10] N.H. Lee, S.Y. Yoon, D.H. Kim, S.K. Kim, B.J. Choi, Electronic Materials Lett. **13**, 318 (2017).

[11] D.H. Kim, D.-Y. Shin, Y.-G. Lee, G.-H. An, J.H. Han, H.-J. Ahn, B.J. Choi, Ceram. Inter. **44**, 19554 (2018).

[12] D. Kim, D.H. Kim, D.-H. Riu, B.J. Choi, Arch. Metall. Mater. **63**, 1061 (2018).